Appendix S1: Description of the pollen, acorn and weather databases

Our spatially extended field networks, including sites experiencing diverse weather conditions, is composed of two databases independently acquired: one with 44 pollen-sampling sites (Fig. S1 and Table S1) (i.e., with at least 8-year recordings available between 1994 and 2015) and the other one with 30 acorn-sampling sites spreading over 790 km in latitude and 850 km in longitude (Fig. S2 and Table S2) and surveyed every year for 14 years (1994-2007).

1) Pollen database

Amounts of airborne pollen (i.e., the estimated number of pollen grains per cubic meter of air) were collected daily throughout the year at every site by the RNSA (Réseau National de Surveillance Aérobiologique, France) between 1994 and 2015 using Hirst traps (Hirst 1952). Data were discarded some years when no successful recording could be made more than 5 consecutive days within the peak of the pollen release (about 15 days centered on the median date of pollen release period).

2) Acorn database

The oak acorn census database has been collected from long-term surveys achieved by the European network for the monitoring of forest ecosystems (RENECOFOR) (Ulrich 1995). Acorn production was analyzed in 30 oak forests distributed across metropolitan France and surveyed from 1994 to 2007 (Fig. S2). Among them, 19 forests were dominated by *Q. petraea*, 9 by *Q. robur* and two of them were mixed oak forests (Table S2). All of these populations were already mature when they started to be monitored. The acorn production was sampled each year of the 14-year survey on a fixed 1-acre surface where ten non-neighboring trees were equipped with one 0.5m^2 raised litter fall trap that collected the mature acorns and prevented them from being eaten. At each site, the acorns fallen into these ten devices were gathered and counted exhaustively.

3) Combining the data of *Quercus petraea* and *Q. robur*

Data concerning these two white oak species were pooled both for our empirical and modeling approach for estimating the model parameters due to the following reasons:

- pollen morphology does not allow discriminating these two *Quercus* species
- the two oak species show the same trend between acorn production and April Temperature (AT) (Table S3 and Fig. S3)
- the population coefficient of variation (CVp) did not significantly differ between the two oak species (*Q. robur*: 1.37 ± 0.31 (mean CVp $\pm$ SD); *Q. petraea*: 1.39 ± 0.37, Student's t-test: $t = 0.18$; $df = 19$; $p = 0.85$)

4) Weather database

To characterize the weather conditions occurring at each sampling site (pollen- and acorn-), mean daily temperature (°C) and cumulated daily rainfall (mm) values were extracted from the SAFRAN (Système d'Analyse Fournissant des Renseignements Adaptés à la Nivologie, Durand *et al.* 1993) spatially-explicit database (a grid with 8×8 km mesh size).

Hirst, J. (1952). An automatic volumetric spore trap. *Ann. Appl. Biol.*, 39(2), 257–265.

Durand, Y., Brun, E., Mérindol, L., Guyomarc'h, G., Lesaffre, B., & Martin, E. (1993). A meteorological estimation of relevant parameters for snow models. *Ann. Glaciol*, 18, 65-71.

Ulrich, E. (1995). Le réseau RENECOFOR: objectifs et réalisation. *Rev. For. Fr.* 47,107–124.

Appendix S2: Evaluation of the method described in Lebourgeois *et al.* (2018) to estimate airborne pollen amount or pollen synchrony at a given site

We evaluated the accuracy of the method used in Lebourgeois *et al.* (2018) to estimate at a given site the annual airborne pollen amount and pollen synchrony (i.e., the duration (days) of the pollen release period) from data collected on neihgbouring sites. For that purpose, we applied their method on 32 pollen-sampling sites for which pollen variables have been recorded at least four years during the 1994-2007 period, and compared the observed and estimated data. For each pollen-sampling site, we proceeded as follows: (i) we estimated the daily pollen aerial concentration as the inverse-distance weighted average concentration measured in all pollen-sampling sites distant by less than 100 km of the focused site; (ii) for each *site·year* combinations we calculated the annual airborne pollen amount (i.e., cumulated daily pollen aerial concentration) and the duration (days) of the pollen release period (i.e., the interquantile range 5%-95%, as in Lebourgeois *et al.* (2018)); (iii) for each site, we calculated the percentage of error $100 \times abs(\frac{\text{estimated data} - \text{observed data}}{\text{observed data}})$, and the number of years with over and underestimation, respectively (see Table S4). The error of estimation was high and highly variable between sites: for the amount of airborne pollen it reached 95.55% on average (minimum = 19.17%; maximum = 479.51%), and for pollen synchrony it averaged 29.59% (minimum = 8.92%; maximum = 84.72%). The amplitude of the estimation bias (over or under) depends on the site, and both under- and over-estimations were often detected at the same site. Considering the acorn-sampling sites, and based on the method of Lebourgeois *et al.* (2018), we computed for each acorn-sampling site the number of pollen-sampling sites available for the estimation of pollen data on that site, including any pollen-sampling site for which pollen had been recorded at least one year among the 14-year acorn survey (1994-2007). Using this non-restrictive criterion, we found 2.27 pollen-sampling sites per acorn-sampling site, on average, and from these ones we were able to estimate the annual airborne pollen amount for only 8.7 years, on average, of the 14-year acorn survey. One major problem was that the pollen and acorn years of survey did poorly overlap. It follows that only 1.46 pollen-sampling site could actually be used each year, on average, at every acorn-sampling sites. Most importantly, the number and identity of pollen-sampling sites that could be used for annual pollen estimation varied throughout the 1994-2007 period for 83% of the acorn-sampling sites. This inconsistency prevented from keeping high-quality estimations of the dynamics of pollen amount within acorn-sampling sites and its variation between sites over their 14-year survey. It seems from these results that the method of Lebourgeois *et al.* (2018) failed to accurately estimate the airborne pollen amount and the duration (days) of the pollen release period at the acorn-sampling sites, thus preventing from directly crossing annual pollen and acorn amounts from these two databases.

Lebourgeois, F., Delpierre, N., Dufrêne, E., Cecchini, S., Macé, S., Croisé, L., & Nicolas, M. (2018). Assessing the roles of temperature, carbon inputs and airborne pollen as drivers of fructification in European temperate deciduous forests. *Eur. J. For. Res.*, 1-17.

Appendix S3: Identifying the periods when weather variables impact the annual airborne pollen amount and analyzing their effect on fruiting intensity

1) Testing the relation between the yearly airborne pollen amount and the weather variables

Pollen aerial release occurred mainly during April and May in all of the 44 pollen-sampling sites monitored by the RNSA (Réseau National de Surveillance Aérobiologique, France) (Fig. S7). We tested the impact of weather variables on the annual airborne pollen amount (at any given year t) from various time period divisions from June 1st (year $t-1$) to May 31st (year t) at each site and each year. The most robust results, presented below, were obtained from time division per calendar month.

For every calendar months of the studied period, we calculated the mean daily temperature (°C) and cumulated rainfall (mm). Then, we performed a Principal Component Analysis (PCA) on these two weather variables to obtain uncorrelated variables that captured most variability. The first selected Principal Component (PC) (with eigenvalues higher than 1) captured between 52% and 75% of the total variance of both temperature and rainfall variability (Table S5). This first axis so-called 'Weather Index' (WI) was used as explanatory variable in the subsequent analysis. The coordinates of every *site·year* combinations on WI constitute the values of this explanatory variable. In Fig. S8, we illustrated the relationships between the April Weather Index (AWI) (i.e., the only period that was significantly correlated to the airborne pollen amount; Tables S6 and S7) and each of the two original monthly average weather variables.

2) Testing the relation between fruiting intensity and the AWI (April Weather Index)

Fruit- and pollen-sampling sites did not overlap in space (Figs. S1 and S2) and only partly overlapped in time because of several missing years for pollen data between 1994 and 2007 (the time lapse survey of acorns) in some sites. Consequently, finding out whether pollen limitation would be due to weather conditions required testing the hypothesis that AWI, that correlated to the airborne pollen amount (Tables S6 and S7), were also correlated to the fruiting intensity at the acorn-sampling sites. We calculated from the meteorological dataset the mean temperature (°C) and rainfall (mm) during at each acorn-sampling site and each year from 1994 to 2007. We determined the AWI coordinates of these mean weather conditions (*site·year* combinations) with the suprow function from the *ade4* package (Dray & Dufour 2007) of the R free software environment (v.3.4.3, `http://cran.r-project.org`). Then, using the glm.nb function of the *fitdistrplus* package (Delignette-Muller & Dutang 2015), we performed a negative binomial Generalized Linear Model (NB GLM using a log link) with the number of acorns (year t) as dependent variable, the number of acorns the previous year (year $t-1$) and the corresponding AWI coordinates as covariates, and the 'site' and 'year' factors considered as fixed effects (Table S3). Finally, we performed an ANODEV to determine the proportion of the 'site' and 'year' effects that were captured by AWI (Table S9).

Delignette-Muller, M.L., & Dutang, C. (2015). fitdistrplus: An R package for fitting distributions. *J. Stat. Softw.*, 64(4), 1-34.

Dray, S. & Dufour, A-B. (2007). The ade4 package: implementing the duality diagram for ecologists. *J. Stat. Softw.*, 22(4), 1–20.

Appendix S4: Resource Budget Model (RBM)

We developed a RBM largely inspired of Venner *et al.* (2016), that accounts for tree resource dynamics, in which we introduced the effect of spring weather conditions on the amount of pollen available for reproduction. We tested with this model to what extent pollen limitation on fruiting dynamics would be mediated by the resource allocation strategy of trees alone, by spring weather conditions alone, or both.

1) Modeling tree resource dynamics

We modeled a forest composed of a large number of trees of the same species, where each tree x occupies a distinct location on a two-dimensional grid, the trees being regularly distributed on this grid. $S_x(t)$ is the level of internal resource reserves of tree x at the beginning of year t. Every year, each tree accumulated a fixed amount of resources from photosynthesis, Ps. Tree x allocates to flowering a given amount of resources depending on the level of its reserve according to a logistic function $f(S_x(t)+Ps)$. From previous work (Venner *et al.* (2016)) the depletion coefficient (DC) is the product of three biological components ($DC = FA \cdot MFS \cdot FFR$), where:

- FA (Female flower Allocation) is the proportion of resource allocated to female flowers (respectively 1-FA for pollen);
- MFS (Maximum Fruit Set) corresponds to the maximum proportion of pollinated female flowers that successfully mature into fruit without any pollen limitation, and allows accounting for flower abscission or fruit abortion commonly observed in perennial plants and independent of any pollen limitation (Holland *et al.* 2004; Stephenson 1981);
- FFR (Fruiting-to-Flowering resource demand Ratio) corresponds to the ratio of the resources required to produce one mature fruit to that required for one sexually operational female flower.

As in Venner *et al.* (2016)'s study, we set 0.5 as a fixed value for FA, considering that the resource allocation to flowering is equal between the sexes (Norton & Kelly 1998). MFS and FFR values were estimated from a field survey of 117 oak trees belonging to 13 populations distributed throughout metropolitan France (see Venner *et al.* 2016 for more details). From these empirical data, MFS was set to 0.8, and FFR was estimated for each surveyed tree using either dry mass, carbon or nitrogen contents (see Venner *et al.* (2016) for more details). FFR was found to fit a log-normal distribution with a mean value of 12.3 (SD = 1.8). Then, we estimated the DC value for each surveyed tree by calculating the product between these three biological components of which two were estimated empirically. Using the *fitdistrplus* package (Delignette-Muller & Dutang 2015), we found that the estimated DC values best fitted a log-normal distribution (with a mean of 5 and a standard deviation of 1.8). We accounted for the variability in DC values observed among trees by assigning a DC value randomly sampled in this distribution to each tree. Because FA (a component of DC) has been set somewhat arbitrarily, we performed a sensitivity analysis on DC using simulations based on two other distributions ($DC \sim \text{log-}\mathcal{N}(2,1.8)$ and $\text{DC} \sim \text{log-}\mathcal{N}(8,1.8)$), which corresponded to male and female-biased allocation to flowering, respectively. Whatever the DC values tested, the simulated results were qualitatively similar (see Fig. S5 and S6). The amount of resource allocated each year by tree x toward fruiting was then $\text{DC} \cdot f(S_x(t)+Ps)$. Successful fruiting might be followed by large resource depletion, which would force the tree to recover its reserves over several years before flowering again. Overall, the relative resource reserve of the tree x at the onset of year $t+1$, once standardized per Ps unit (the fixed amount of resources gained yearly through photosynthesis), can be computed as follows:

$$Y_x(t+1) = Y_x(t) - f(Sx(t)+Ps)(1+\text{FA}\cdot\text{MFS}\cdot\text{FFR})+1 \text{ accordingly } Y_x = \frac{S_x(t)+Ps}{Ps} \qquad (1)$$

We further enhanced this basic dynamic equation by accounting for out-cross pollination (see section 2) and by introducing environmental stochasticity in the amount of resources acquired yearly by individual trees (i.e., Ps). As a result, equation (1) becomes:

$$Y_x(t+1) = Y_x(t) - f(Sx(t) + Ps)(1 + \mathrm{FA} \cdot \mathrm{MFS} \cdot \mathrm{FFR} \cdot P_x(t)) + \varepsilon_x + 1 \quad (2)$$

where $P_x(t)$ is the pollination success of the tree x, and $\varepsilon_x(t)$ is the error that results from individual tree variation added to population-wide yearly variation (see Satake & Iwasa 2002a for details).

2) The out-cross pollination process

Our RBM included a pollen limitation function (see section 5) precluding self-pollination (Satake & Iwasa 2000), because resource dynamics do not induce fruiting synchrony among trees, and because pollination efficiency overall depends on the amount of out-cross pollen available (Nilsson & Wastljung 1987; Smith *et al.* 1991). The number of acorns produced by a single tree in any given year, therefore, depends not only on the number of female flowers it produces but also on the amount of exogenous pollen available, which itself depends on the number of neighboring trees and on the total amount of pollen they produce (see section 3).

3) Determining the set of neighboring trees that might pollinate a focal tree

The model was spatially explicit with trees regularly distributed on a two-dimensional square grid defined as a tore to avoid edge effects. The distance between two trees located at (x_1, y_1) and (x_2, y_2) respectively, was calculated using the Moore neighborhood method. Any tree distant from the focal tree x by less than a threshold value D could pollinate this tree x; this situation occurred whenever $\max(|x_1 - x_2|, |y_1 - y_2|) \leq \mathrm{D}$. At one extreme case ($\mathrm{D} = 1$), only the eight trees immediately adjacent to the focal tree on the grid could pollinate it, while at the other extreme case, the whole forest could potentially contribute to pollinate the focal tree. How D impacted fruiting had been explored elsewhere (see Satake & Iwasa 2002a), we exclusively considered an intermediate situation where only trees distant, in the sense of Moore, from the focal tree by less than 5 units on the grid (which encompasses 120 neighboring trees) could pollinate it.

4) Determining the relative amount of out-cross pollen available for a focal tree

For each tree, we calculated the relative pollen production, as the ratio of the amount of pollen it actually produced to the maximum amount it would have produced if the level of reserve was equal to the total resources acquired through photosynthesis at the beginning of the focal year. For a given focal tree x, we computed the Pollen Availability Index (PAI, comprised between 0 and 1) as the summed relative pollen produced yearly by its z neighboring trees:

$$\mathrm{PAI}_x(t) = \frac{1}{z} \sum_{y=1}^{z} \max(Y_y(t), 0) \quad (3)$$

5) The pollen limitation function

Following Satake & Iwasa (2000), the pollination success of tree x, $\mathrm{P}_x(t)$, was introduced in the model to account for out-cross pollen limitation on reproduction. In our model, fruiting success depended on a logistic out-cross pollination function linking the amount of out-cross pollen available and pollination success. This means that, at any year t, the probability $\mathrm{P}_x(t)$ for a female flower of tree x to become a mature fruit increases following a logistic function with pollen availability $\mathrm{PAI}_x(t)$. This logistic model allows integrating a dilution and saturation effects at low and high pollen availability, respectively (see Venner *et al.* 2016).

6) Accounting for environmental stochasticity

There is empirical evidence that trees, even when they are distant from each other, reproduce synchronously partly because they experience similar environmental fluctuations (Koenig & Knops 1998; Koenig & Knops 2000; Koenig & Knops 2013). As did Satake & Iwasa (2002b), an environmental noise $\varepsilon_x(t)$ was introduced into our model to account for the fact that the resources gained from photosynthesis by the tree x may differ from one year to the next, due to (i) climatic variations that evenly affect all the trees in the population and (ii) to fine-scale environmental differences (e.g., soil characteristics, available nutrients, water supply) exclusively affecting the tree x. Here, $\varepsilon_x(t)$ accounts for individual stochastic variation in the resources accumulated by the tree x at the onset of the reproductive season t; it can depart from the average population noise ε_{pop} which itself may vary from one year to the next, so that:

$$\varepsilon_x(t) \sim \mathcal{N}(\varepsilon_{pop}, \sigma_{env}\sqrt{1-\mathrm{Sy}_{env}}) \text{ with } \varepsilon_{pop} \sim \mathcal{N}(0, \sigma_{env}\sqrt{\mathrm{Sy}_{env}}) \tag{4}$$

Sy_{env} is the environmental synchrony among trees and is defined as the proportion of the total environmental variance (σ^2_{env}) due to population-scale variance. The Moran effect has been well studied elsewhere (see Satake & Iwasa 2002a), so in our model, we fixed intermediate values for σ_{env} and Sy_{env} (0.2 and 0.5, respectively). Environmental stochasticity, by affecting the resources gained by trees, indirectly impacts the amount of out-cross pollen produced yearly. We then modified equation (3) to introduce this stochasticity into the pollen availability index as followed:

$$\mathrm{PAI}_x(t) = \frac{1}{\sum_{y=1}^{z}[1+\varepsilon_y(t-1)]} \sum_{y=1}^{z} \max(Y_y(t), 0) \tag{5}$$

7) Pollen available for pollination: accounting for spring weather conditions

Each year, a April mean Temperature (AT) value (or April Weather Index, AWI) was drawn from a normal distribution established empirically for each site (see section 8). From the AT value (or AWI value), a coefficient weighting pollen release and aerial diffusion called hereafter 'Pollen Diffusion Coefficient' (PDC) between 0 and 1 was defined for a given year and allowed correcting downward he amount of out-cross pollen available for trees. PDC was logistically related to AT as follows:

$$\mathrm{PDC} = 0.45 + \frac{0.55}{1+\mathrm{e}^{-1.4\cdot(\mathrm{AT}-11.5)}} \tag{6}$$

This logistic function (equation 6) allowed taking into account the best-fitted logistic relationship between the airborne pollen amount and the AT (Fig. 3a) and to ensure that PDC tended toward 1 when the weather conditions tended toward optimal weather conditions for aerial pollen diffusion (i.e., the AT values tend toward infinity). Finally, the PAI calculated in equation (5) became:

$$\mathrm{PAI}_x(t) = \mathrm{PAI}_x(t) \cdot \mathrm{PDC} \tag{7}$$

For each tree x, the Resource Allocation towards Fruiting (RAF) can be calculated, as follows:

$$\mathrm{RAF} = \mathrm{FA} \cdot \mathrm{MFS} \cdot \mathrm{FFR} \cdot f(S_x(t) + Ps) \cdot \mathrm{P}_x(t) \tag{8}$$

Assuming that the number of fruits cannot realistically tend toward infinity, a saturation function for RAF was introduced in such a way that a tree cannot allocate more than 5 times the entire resources acquired, on average, in a given year by photosynthesis:

$$\mathrm{RAF}_{\mathrm{corrected}} = \frac{\mathrm{RAF}}{\mathrm{RAF}/(10+1)} \tag{9}$$

Then equation (2) of our RBM became:

$$Y_x(t+1) = Y_x(t) - f(S_x(t) + Ps) - \mathrm{RAF}_{\mathrm{corrected}} + \varepsilon_x(t) + 1 \tag{10}$$

8) Simulating multiple tree populations: accounting for variability between tree populations in the spring weather and pollen limitation

Using the tree population model described above, we simulated a set of 44 distinct populations (similar number to empirical survey pollen-sampling sites). First, to account for the variability observed among tree populations in the AT (or AWI) values, we established for each of the 44 distinct tree populations its specific AT (or AWI) normal distribution in which the AT (or AWI) value was randomly selected each year. For this purpose, we calculated for each of our 44 empirical pollen-sampling sites (Fig. S1 and Table S1) the mean temperature (°C) and rainfall (mm) during April for each year from 1959 to 2012, using the daily meteorological data from the SAFRAN application (see Appendix S1). Then, we determined the corresponding coordinates of these mean weather conditions (*site·year*) on the AT (or AWI) using the suprow function from the *ade4* package (Dray & Dufour 2007) of the R free software environment (v.3.4.3, `http://cran.r-project.org`). Finally, we fitted a normal distribution for the AT (or AWI) for each given pollen-sampling sites using the fitdist function from the *fitdistrplus* package (Delignette-Muller & Dutang 2015), and implemented them in our model. Second, because a Variability of Pollination Efficiency (VPE) can occur between sites independently of the weather conditions (e.g., in function of tree density), we introduced this source of variation in the model (see Venner *et al.* 2016) for sensitivity analysis of masting to pollination efficiency). For each of the 44 simulated tree populations, the pollination success $P_x(t)$ varied following a logistic function with the pollen availability $PAI_x(t)$, as follows:

$$P_x(t) = \frac{1}{1 + \text{VPE} \cdot e^{-12 \cdot PAI_x(t)}} \text{ with VPE } \sim \text{log-}\mathcal{N}(6, 1.5) \quad (11)$$

9) Model processing and model outputs: pollen and fruit population Coefficient of Variation (CVp) and relative amount of pollen available for reproduction and fruit allocation as a function of April mean Temperature (AT)

In our model, we used a square grid of 400 trees. All simulations were run following an algorithm developed in `C++`. Each simulation lasted 2,000 time steps (years), but only the last 20 years (as for our empirical data about acorns) were used to gather data similar to those got on the survey pollen- and acorn-sampling sites (i.e., annual amount of airborne pollen and fruit production at the population-scale, and the AT (or AWI) for each of the 20 years). Then, as for empirical data, we calculated the following descriptors: pollen- and fruit-CVp, the annual airborne pollen amount and fruit production relative to the maximum value encountered on that site for 20 years. From these simulated data, we displayed the cumulative frequency curves from the 44 pollen- and fruit-CVp, and the mean relationships between the AT (or AWI) and the relative amount of pollen available for reproduction, and allocation to fruiting respectively. Finally, we ran 100 simulations for each of the 44 simulated population-sites and we drawn the 95% credible interval.

10) Testing different types of pollen limitation

We tested four distinct scenarios relative to the pollen limitation hypothesis: (i) no pollen limitation (P_x = MFS regardless PAI) (Fig. 4a,e,i); (ii) pollen limitation due to both weather conditions and resource allocation strategy to flowering (Fig. 4d,h,l); (iii) 'resource-driven pollen limitation', that is, limitation exclusively depending on the way trees allocate their resource to flowering, while weather conditions are constant and optimal (i.e., PDC = 1) (Fig. 4b,f,j); (iv) 'weather-driven pollen limitation', that is, limitation exclusively depending on the sensitivity of aerial pollen diffusion to spring weather conditions (i.e., the resource allocated to female flowers depends on the level of the tree reserve, but pollen production is constant) (Fig. 4c,g,k).

11) Computing

We simulated a set of 44 populations (i.e., as many as the number of pollen-sampling sites) each of these being provided with its own weather characteristics (i.e., the empirical AT distribution; Appendix S3). We repeated 100 simulations for each set of 44 populations with a `C++` algorithm. Each simulation lasted 2,000 time steps (years), but only the last 20 steps (same time scale as the 22-year survey pollen data and the 14-years survey fruit data, and independent from initial conditions) were used to compute the population Coefficient of Variation (CVp) at each site for the relative airborne pollen amount and fruit abundance, with their corresponding simulated AT values. These values were shown with their 95% credible interval. (i.e., interval including 95% of the simulations).

Delignette-Muller, M.L., & Dutang, C. (2015). fitdistrplus: An R package for fitting distributions. *J. Stat. Softw.*, 64(4), 1-34.

Dray, S. & Dufour, A-B. (2007). The ade4 package: implementing the duality diagram for ecologists. *J. Stat. Softw.*, 22(4), 1–20.

Holland, J.N., Bronstein, J.L. & DeAngelis, D.L. (2004). Testing hypotheses for excess flower production and low fruit-to-flower ratios in a pollinating seed-consuming mutualism. *Oikos*, 105(3), 633–640.

Koenig, W.D. & Knops, J.M. (1998). Scale of mast-seeding and tree-ring growth. *Nature*, 396(6708), 225–226.

Koenig, W.D. & Knops, J.M. (2000). Patterns of annual seed production by northern hemisphere trees: a global perspective. *Am. Nat.*, 155(1), 59–69.

Koenig, W.D. & Knops, J.M. (2013). Large-scale spatial synchrony and cross-synchrony in acorn production by two California oaks. *Ecology,* 94(1), 83–93.

Nilsson, S.G. & Wastljung, U. (1987). Seed predation and cross-pollination in mast-seeding beech (*Fagus sylvatica*) patches. *Ecology*, 68(2), 260–265.

Norton, D.A., & Kelly, D. (1988). Mast seeding over 33 years by Dacrydium cupressinum Lamb.(rimu) (Podocarpaceae) in New Zealand: the importance of economies of scale. *Funct. Ecol.,* 399-408.

Satake, A. & Iwasa, Y. (2000). Pollen coupling of forest trees: forming synchronized and periodic reproduction out of chaos. *J. Theor. Biol.*, 203(2), 63–84.

Satake, A. & Iwasa, Y. (2002a). The synchronized and intermittent reproduction of forest trees is mediated by the Moran effect, only in association with pollen coupling. *J. Ecol., 90(5),* 830–838.

Satake, A. & Iwasa, Y. (2002b). Spatially limited pollen exchange and a long-range synchronization of trees. *Ecology,* 83(4), 993–1005.

Smith, C.C., Hamrick, J. & Kramer, C.L. (1990). The advantage of mast years for wind pollination. *Am. Nat.*, 136(2), 154–166.

Stephenson, A. (1981). Flower and fruit abortion: proximate causes and ultimate functions. *Annu. Rev. Ecol. Syst.*, 12(1), 253–279.

Venner, S., Siberchicot, A., Pélisson, P-F., Schermer, E., Bel-Venner, M-C., Nicolas, M. et al. (2016). Fruiting strategies of perennial plants: a resource budget model to couple mast seeding to pollination efficiency and resource allocation strategies. *Am. Nat.,* 188(1), 66–75.

Table S1: The GPS coordinates of the 44 pollen-sampling sites located across metropolitan France and recorded from 1994 to 2015 by the RNSA (Réseau National de Surveillance Aérobiologique, France).

Number	Latitude	Longitude	Cities
1	44.20	0.63	Agen
2	49.90	2.30	Amiens
3	47.46	-0.55	Angers
4	45.65	0.15	Angoulême
5	46.20	6.25	Annemasse
6	43.48	-1.48	Bayonne
7	46.20	5.21	Bourg-en-Bresse
8	46.78	4.85	Chalon-sur-Saône
9	45.56	5.93	Chambéry
10	45.78	3.08	Clermont-Ferrand
11	46.66	-1.43	La Roche-sur-Yon
12	48.68	6.20	Nancy
13	46.98	3.16	Nevers
14	47.92	1.90	Orléans
15	46.58	0.33	Poitiers
16	48.06	-2.98	Pontivy
17	49.25	4.03	Reims
18	48.08	-1.68	Rennes
19	49.43	1.08	Rouen
20	45.37	4.81	Roussillon
21	48.58	7.75	Strasbourg
22	43.60	1.43	Toulouse
23	45.90	6.11	Annecy
24	44.91	2.45	Aurillac
25	47.25	6.03	Besançon
26	44.83	-0.56	Bordeaux
27	49.18	-0.35	Caen
28	43.60	2.25	Castres
29	47.06	-0.88	Cholet
30	48.00	-2.00	Dinan
31	45.16	5.71	Grenoble
32	50.63	3.06	Lille
33	45.75	4.85	Lyon
34	49.13	6.16	Metz
35	46.33	2.60	Montluçon
36	47.21	-1.55	Nantes
37	48.86	2.33	Paris
38	43.30	-0.36	Pau
39	45.18	0.71	Périgueux
40	46.17	-1.15	La Rochelle
41	48.49	-2.75	Saint-Brieuc
42	45.42	4.39	Saint-Étienne
43	47.38	0.68	Tours
44	48.30	4.08	Troyes

Table S2: Characteristics of the 30 acorn-sampling sites widespread across metropolitan France and surveyed from 1994 to 2007 by the ONF (Office National des Forêts, France). The acorn-sampling sites are indexed on the map (Fig. S2) by their number indicated in the column 'Number'. The GPS coordinates and the altitude are indicated in the corresponding columns 'Latitude', 'Longitude', and 'Altitude (m)'. The number of trees sampled to determine the relative abundance of each species within forest stands is indicated in the column 'Number of sampled trees'. The associated columns '*Q. robur* (%)' and '*Q. petraea* (%)' correspond to the relative percentage of these two oak species in the forest stand.

Number	Latitude	Longitude	Altitude (m)	Number of sampled trees	*Q. robur* (%)	*Q. petraea* (%)
1	46.17	5.24	260	102	0	100
2	46.67	2.73	260	95	0	100
3	48.30	4.46	160	89	3	97
4	47.25	2.12	176	93	0	100
5	47.08	5.08	220	84	2	98
6	49.37	1.50	175	74	0	100
7	48.18	-1.53	80	76	1	99
8	47.57	1.26	127	99	0	100
9	49.03	4.96	180	61	0	100
10	48.87	6.48	315	79	0	100
11	49.02	7.46	320	116	0	100
12	46.97	3.66	270	93	0	100
13	49.40	2.30	55	60	12	88
14	48.52	0.68	220	108	0	100
15	47.69	7.47	256	56	0	100
16	47.80	0.38	170	129	0	100
17	44.05	1.75	300	121	0	100
18	46.63	0.50	116	100	0	100
19	48.03	6.04	330	72	0	100
20	48.35	4.30	115	77	100	0
21	43.74	-0.84	20	128	98	2
22	47.46	0.03	57	87	100	0
23	49.02	5.77	220	67	100	0
24	50.17	3.75	149	57	100	0
25	43.20	-0.04	370	70	100	0
26	47.87	6.21	240	116	100	0
27	46.97	5.24	190	145	100	0
28	46.83	2.57	175	75	100	0
29	48.99	7.73	350	unknown	unknown	unknown
30	48.45	2.72	80	52	48	52

Table S3: Summary of different negative binomial Generalized Linear Models (NB GLMs using a log link) considering the 'year' and 'site' as fixed effects for predicting the acorn abundance the year t (Fruit t). The significant variables are in bold characters. Neither the species factor nor the interaction *species* $\times$ *weather variable* (April temperature (AT) or April Weather Index (AWI)) had significant effect on acorn production. Consequently, the two selected models for predicting the acorn abundance the year t are: (i) Fruit t ~ Fruit $t-1$ + year + site + AWI and (ii) Fruit t ~ Fruit $t-1$ + year + site + AT.

	Covariates	Estimates	SE	z-value	Pr(>|z|)
April Weather Index (AWI)					
	(Intercept)	5.32	0.52	10.23	< 2e-16
	Fruit $_{t-1}$	**-0.0014**	**0.00048**	**-2.84**	**0.0045**
	Species	0.76	0.57	1.33	0.19
	AWI	**0.74**	**0.19**	**3.75**	**0.00017**
	Species $\times$ AWI	0.13	0.15	0.82	0.41
April Temperature (AT)					
	(Intercept)	-2.96	1.63	-1.81	0.069
	Fruit $_{t-1}$	**-0.0013**	**0.00048**	**-2.86**	**0.0042**
	Species	2.08	1.34	1.56	0.12
	AT	**0.87**	**0.19**	**4.66**	**3.15e-06**
	Species $\times$ AT	-0.14	0.12	-1.10	0.27
Selected model with AWI					
	(Intercept)	6.07	0.47	12.84	< 2e-16
	Fruit $_{t-1}$	**-0.0013**	**0.00046**	**-2.89**	**0.0038**
	AWI	**0.67**	**0.18**	**3.70**	**0.00022**
Selected model with AT					
	(Intercept)	-1.17	1.66	-0.70	0.48
	Fruit $_{t-1}$	**-0.0013**	**0.00046**	**-2.89**	**0.0038**
	AT	**0.75**	**0.18**	**4.29**	**1.74e-05**

Table S4: Evaluation of the method used by Lebourgeois *et al.* (2018) for estimating the annual airborne pollen amount and pollen synchrony (i.e., duration (number of days) of pollen release period) at each of the acorn sampling-sites from pollen data recorded at sampling sites distant by less than 100 km. Here, for the purpose of comparing estimated and empirical values, we applied their method at pollen- instead of acorn-sampling sites (see Appendix S2 for more details). 'Focal sites' corresponds to the pollen-sampling sites for which pollen variables have been both recorded and estimated, at least four years during the 1994-2007 period (the code name used here is the one used by the Réseau National de Surveillance Aérobiologique: `http://www.pollens.fr`); '#sites' corresponds to the number of neighboring pollen-sampling sites (within a 100 km radius as for Lebourgeois *et al.* (2018)) available to estimate the daily airborne pollen on the focal pollen-sampling; 'Error (%)' corresponds to the annual average percentage of error between observed and estimated data (i.e., $100 \times abs(\frac{\text{estimated data} - \text{observed data}}{\text{observed data}})$. The number of years with underestimation and overestimation are indicated in the columns 'Under' and 'Over', respectively. The last line in bold letter shows the mean values for the columns '#sites' and 'Error (%)', and the sum for the columns 'Focal sites', 'Under' and 'Over'.

		Airborne pollen amount			Pollen synchrony		
Focal sites	#sites	Error (%)	Under	Over	Error (%)	Under	Over
FRAGEN	1	28.67	4	1	21.86	4	1
FRAIXP	4	215.31	0	5	23.59	3	2
FRANNE	3	57.42	4	7	45.88	4	7
FRAURI	1	62.81	11	0	39.96	1	10
FRBESA	1	55.51	2	3	12.29	1	4
FRBRIA	3	479.51	0	6	22.76	4	2
FRCAEN	1	220.11	1	6	24.92	5	2
FRCHAL	1	21.00	9	2	14.61	10	1
FRCHAM	6	17.62	2	4	16.15	3	3
FRCHOL	3	44.59	3	7	41.15	4	6
FRDIJO	2	19.17	2	4	19.84	0	6
FRDINA	3	31.80	4	1	20.20	2	3
FRFONT	2	326.00	3	5	26.41	3	5
FRGREN	6	127.47	0	9	84.72	2	7
FRLAFE	1	62.82	6	1	52.51	1	6
FRLARO	3	82.04	6	1	12.25	2	5
FRLILL	2	105.82	1	11	34.26	7	5
FRLYON	4	44.55	8	1	11.06	5	4
FRMARS	4	77.68	1	9	15.36	4	6
FRMONP	2	177.88	0	5	31.56	5	0
FRMONT	3	65.22	11	0	8.92	4	7
FFRNANT	4	98.72	1	8	21.44	8	1
FRNEVE	1	61.94	1	3	13.58	2	2
FRNIME	4	63.97	10	0	51.22	0	10
FRPERP	2	123.26	5	3	24.45	5	3
FRPOIT	1	29.58	1	3	31.46	4	0
FRPONT	3	63.04	0	5	16.61	4	1
FRRENN	4	74.05	2	2	51.25	0	4
FRROCH	1	62.95	1	7	42.18	8	0
FRROUE	1	34.20	13	1	59.70	3	11
FRSTET	2	71.17	1	8	27.90	0	9
FRTOUN	2	52.01	0	4	27.06	4	0
N=32	**2.53**	**95.55**	**113**	**132**	**29.59**	**112**	**133**

Table S5: Proportion of variance explained by each of Weather Index (i.e., the first axis of the Principal Component Analysis (PCA) performed on mean temperature (°C) and rainfall (mm) for each month) used as covariates in the Generalized Linear Mixed Models (GLMMs with Gaussian family and identity link) for predicting annual airborne pollen amount and pollen synchrony (i.e., the interquartile range in number of days of the cumulated daily airborne pollen amount) the year t.

Weather Index	Proportion of variance explained (%)	Weather variables captured
June Weather Index $_{t-1}$	53.89	temperature (+) and rainfall (-)
July Weather Index $_{t-1}$	65.09	temperature (+) and rainfall (-)
August Weather Index $_{t-1}$	65.99	temperature (+) and rainfall (-)
September Weather Index $_{t-1}$	55.43	temperature (+) and rainfall (-)
October Weather Index $_{t-1}$	52.69	temperature (+) and rainfall (+)
November Weather Index $_{t-1}$	66.94	temperature (-) and rainfall (-)
December Weather Index $_{t-1}$	69.82	temperature (+) and rainfall (+)
January Weather Index $_{t}$	73.45	temperature (-) and rainfall (-)
February Weather Index $_{t}$	72.82	temperature (-) and rainfall (-)
March Weather Index $_{t}$	55.48	temperature (+) and rainfall (-)
April Weather Index $_{t}$ (AWI $_{t}$)	67.56	temperature (+) and rainfall (-)
May Weather Index $_{t}$	59.26	temperature (+) and rainfall (-)

Table S6: Summary of the Generalized Linear Mixed Model (GLMM with Gaussian family and identity link) performed on the screening dataset and selected using Akaike Information Criterion (AIC) and model averaging thanks to the pdredge function of the *MuMIn* package[1] of the R free software environment (v.3.4.3, `http://cran.r-project.org`) for predicting annual airborne pollen amount and pollen synchrony (i.e., the interquartile range in number of days of the cumulated daily airborne pollen amount) the year t. Only the weather variables that were included in the GLMMs associated to a delta AIC less than 2 are shown in the table. The significant variables are in bold characters.

Dependent variable	Weather covariates	Estimates	SE	t-value	Pr(>|t|)
Airborne pollen amount $_t$					
	(Intercept)	8.08	0.21	37.42	$< 10^{-16}$
	June Weather Index $_{t-1}$	-0.027	0.040	0.67	0.49
	July Weather Index $_{t-1}$	-0.059	0.042	1.41	0.16
	August Weather Index $_{t-1}$	-0.034	0.040	1.02	0.40
	October Weather Index $_{t-1}$	0.026	0.043	0.59	0.55
	November Weather Index $_{t-1}$	-0.084	0.051	1.65	0.099
	December Weather Index $_{t-1}$	-0.072	0.049	1.49	0.14
	January Weather Index $_t$	0.022	0.041	0.54	0.59
	April Weather Index $_t$ (AWI $_t$)	**0.13**	**0.045**	**2.83**	**0.0046**
	May Weather Index $_t$	0.070	0.039	1.79	0.07
Pollen synchrony $_t$					
	(Intercept)	2.29	0.069	33.19	$< 10^{-16}$
	June Weather Index $_{t-1}$	-0.019	0.035	0.539	0.59
	July Weather Index $_{t-1}$	0.032	0.037	0.869	0.39
	August Weather Index $_{t-1}$	0.022	0.034	0.654	0.51
	September Weather Index $_{t-1}$	**-0.11**	**0.037**	**2.93**	**0.0034**
	October Weather Index $_{t-1}$	**0.091**	**0.038**	**2.37**	**0.018**
	December Weather Index $_{t-1}$	0.045	0.038	1.19	0.23
	January Weather Index $_t$	-0.059	0.037	1.60	0.11
	February Weather Index $_t$	0.063	0.039	1.61	0.11
	March Weather Index $_t$	**0.12**	**0.039**	**3.26**	**0.0011**
	April Weather Index $_t$	-0.053	0.038	1.39	0.16

[1] Burnham, K.P. & Anderson, D.R. (2002). *Model selection and multimodel inference*: *a practical information-theoretic approach.* 2nd ed. New York, Springer Verlag.

Table S7: Summary of the Generalized Linear Model (GLM with Gaussian family and identity link), performed on the validation dataset, for predicting the annual airborne pollen amount and pollen synchrony (i.e., the interquartile range in number of days of the cumulated daily airborne pollen amount) the year t (see Table S6 for a summary of the weather variables identified in the selected Generalized Linear Mixed Model (GLMM with Gaussian family and identity link) performed on the screening dataset). The significant variables are in bold characters.

Dependent variable	Weather covariates	Estimates	SE	t-value	Pr(>|t|)
Airborne pollen amount $_t$					
	(Intercept)	8.88	0.34	26.10	$< 10^{-16}$
	Airborne pollen amount $_{t-1}$	**-0.15**	**0.046**	**-3.21**	**0.0015**
	April Weather Index $_t$ **(AWI** $_t$**)**	**0.25**	**0.057**	**4.40**	**1.61e-05**
Pollen synchrony $_t$					
	(Intercept)	2.42	0.23	10.45	$< 10^{-16}$
	September Weather Index $_{t-1}$	-0.037	0.045	-0.82	0.41
	October Weather Index $_{t-1}$	-0.048	0.049	-0.87	0.37
	March Weather Index $_t$	0.077	0.055	1.40	0.16

Table S8: Analysis of deviance (ANODEV) performed from the Generalized Linear Model (GLM with Gaussian family and identity link) for the annual airborne pollen amount and pollen synchrony (i.e., the interquartile range in number of days of the cumulated daily airborne pollen amount) predicted the year t. The proportion of the 'year' and 'site' effects that are captured by the Weather Index (WI) are indicated in the lines 'site' and 'year', respectively. These proportions have been calculated as $\frac{Dev_{mod3}-Dev_{mod2}}{Dev_{mod3}-Dev_{mod1}}$ and as $\frac{Dev_{mod5}-Dev_{mod4}}{Dev_{mod5}-Dev_{mod1}}$ respectively, where Dev_{modX} is the deviance value associated to the model X (see the model reference numbers in the table). The part of observed variation in the airborne pollen amounts that is explained by the 'year', 'site' and WI is indicated in the corresponding columns.

	Models	Df	Resid. Df	Deviance	Resid. Dev	$R^2(\%)$	year (%)	site (%)	WI (%)
Airborne pollen amount $_t$							10.6	36.4	12.8
	NULL		270		192.66				
	Pollen $_t$ ~ Pollen $_{t-1}$	1	269	34.10	158.56	17.70			
	Pollen $_t$ ~ Pollen $_{t-1}$ + year + site	41	229	145.60	47.05	75.57			
	(1) Pollen $_t$ ~ Pollen $_{t-1}$ + year + site + WI $_t$	42	228	149.29	43.37	77.50			
	(2) Pollen $_t$ ~ Pollen $_{t-1}$ + year + WI $_t$	21	249	75.35	117.31	39.11			
	(3) Pollen $_t$ ~ Pollen $_{t-1}$ + year	20	250	74.97	117.69	38.91			
	(4) Pollen $_t$ ~ Pollen $_{t-1}$ + site + WI $_t$	23	247	135.32	57.34	70			
	(5) Pollen $_t$ ~ Pollen $_{t-1}$ + site	248	22	121.29	71.37	63			
	WI $_t$ (i.e., April Weather Index)								1.93
	year								50.11
	site								0.52
Pollen synchrony $_t$							13.30	43.64	3.51
	NULL		270		616.13				
	Synchrony $_t$ ~ year + site	40	230	350.87	265.25	56.94			
	(1) Synchrony $_t$ ~ year + site + WI $_t$	43	227	361.21	254.91	58.62			
	(2) Synchrony $_t$ ~ year + WI $_t$	22	248	100.35	515.77	16.28			
	(3) Synchrony $_t$ ~ year	19	251	81.97	534.15	13.30			
	(4) Synchrony $_t$ ~ site + WI $_t$	24	246	163.79	452.33	26.58			
	(5) Synchrony $_t$ ~ site	21	249	132.71	483.41	21.53			
	WI $_t$ (i.e., September WI, October WI and March WI)								1.68
	year								13.60
	site								0.065

Table S9: Analysis of deviance (ANODEV) performed from the negative binomial Generalized Linear Model (NB GLM using a log link) predicting the acorn abundance the year t (Fruit $_t$). The proportion of the 'site' and 'year' effects that was captured by the April Weather Index (AWI) is indicated in the lines 'site' and 'year', respectively. These proportions have been calculated as $\frac{Dev_{mod3}-Dev_{mod2}}{Dev_{mod3}-Dev_{mod1}}$ and as $\frac{Dev_{mod5}-Dev_{mod4}}{Dev_{mod5}-Dev_{mod1}}$ respectively, where Dev_{modX} is the deviance value associated to the model X (see the model reference numbers in the table). The part of observed variation in the airborne pollen amounts that is explained by the 'year', 'site' and AWI is shown in the corresponding columns.

	Models	Df	Resid. Df	Deviance	Resid. Dev	R^2	year (%)	site (%)	AWI (%)
Fruit $_t$							7.11	7.23	7.35
	NULL		389		606.69				
	Fruit $_t$ ~ Fruit $_{t-1}$	1	388	2.47	604.22	0.4			
	Fruit $_t$ ~ Fruit $_{t-1}$ + year + site	42	347	115.54	491.15	19.04			
	(1) Fruit $_t$ ~ Fruit $_{t-1}$ + year + site + AWI $_t$	43	346	131.60	475.09	21.69			
	(2) Fruit $_t$ ~ Fruit $_{t-1}$ + year + AWI $_t$	14	375	73.95	532.74	12.18			
	(3) Fruit $_t$ ~ Fruit $_{t-1}$ + year	13	376	63.30	543.39	10.48			
	(4) Fruit $_t$ ~ Fruit $_{t-1}$ + site + AWI $_t$	31	358	66.26	540.43	10.92			
	(5) Fruit $_t$ ~ Fruit $_{t-1}$ + site	30	359	33.37	573.32	5.50			
	AWI $_t$								2.64
	year								33.48
	site								15.59

Table S10: Model selection using the Akaike Information Criterion (AIC) between the logistic model and polynomial regression models of degree 1, 2 and 3 for the relationship between the means of April Weather Index (AWI) (or means of April Temperature (AT)) and means of pollen (i.e., yearly amount of oak airborne pollen) (see *Pollen* columns), and means of fruit (acorn abundance) (see *Fruit* columns). For pollen, data collected yearly for 22 years at each of the 44 sites were ranked according to their corresponding AWI (or AT) values, then sets of 14 consecutive values were made to compute means of airborne pollen amount (in all 518 *site·year* combinations available). The same was done for acorn data (in all 420 *site·year* combinations available), except that means were computed on sets of 12 consecutive values. Logistic regression was the best model (bold characters) to describe the mean relationships between AWI (or AT) and pollen (Fig. 3a) and between AWI (or AT) and oak acorns (Fig. 3b).

Models	AWI		AT	
	Pollen	*Fruit*	*Pollen*	*Fruit*
Logistic	**-120.55**	**-56.17**	**-92.38**	**-78.52**
First order polynomial	-97.17	-47.89	-81.49	-63.98
Second order polynomial	-104.96	-55.55	-79.91	-70.04
Third order polynomial	-109.21	-54.27	-91.88	-77.69

Table S11: Summary of the Generalized Linear Mixed Model (GLMM with Gaussian family and identity link) with the amount of airborne pollen as the log-transformed dependent variable and pollen synchrony (i.e., the interquartile range 25%-75% in number of days of the cumulated daily airborne pollen amount) the year t as covariate, and with the 'site' and 'year' factors as random effects.

Covariates	Estimates	SE	t-value	Pr(>|t|)
(Intercept)	7.86	0.072	107.38	$<10^{-16}$
Pollen synchrony $_t$	0.0073	0.0054	1.34	0.18

Table S12: Summary of the negative binomial Generalized Linear Models (NB GLMs using a log link) predicting the acorn abundance the year t (Fruit $_t$) used to test the effect of the weather variables correlated with pollen synchrony (i.e., the interquartile range in number of days of the cumulated daily airborne pollen amount) (*Model 1*) and the effect of April Weather Index (AWI) correlated with the amount of airborne pollen (*Model 2*). In the '*Model 1*' the dependent variable is the residuals of the following model: Fruit $_t$ ~ Fruit $_{t-1}$ + year + site + AWI $_t$, whereas in the '*Model 2*' the dependent variable is the residuals of the following model: Fruit $_t$ ~ Fruit $_{t-1}$ + year + site + March Weather Index $_t$ + October Weather Index $_{t-1}$ + September Weather Index $_{t-1}$. The significant effects are indicated in bold characters.

	Covariates	Estimates	SE	t-value	Pr(>|t|)
Model 1					
	(Intercept)	0.42	0.050	7.46	$< 10^{-16}$
	March Weather Index $_t$	0.041	0.058	0.71	0.48
	October Weather Index $_{t-1}$	0.064	0.047	1.37	0.17
	September Weather Index $_{t-1}$	-0.052	0.061	-0.88	0.37
Model 2					
	(Intercept)	0.40	0.054	7.38	9.6e-13
	AWI $_t$	**0.11**	**0.049**	**2.15**	**0.032**

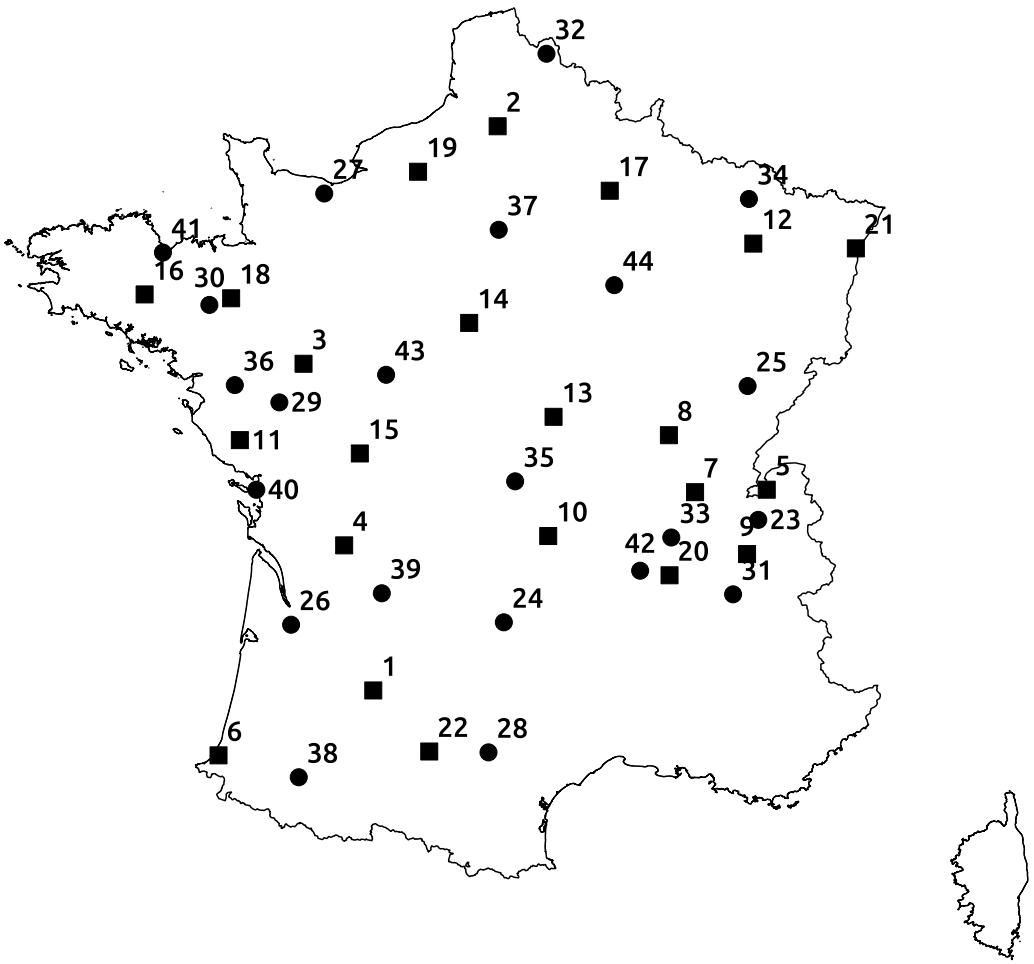

Fig. S1: Spatial distribution of the 44 pollen-sampling sites surveyed by the RNSA (Réseau National de Surveillance Aérobiologique, France). The first 22 survey sites represented by a square symbol were used to identify period and weather variables that were correlated to the annual oak airborne pollen amount or to the pollen synchrony (i.e., the interquartile range in number of days of the cumulated daily airborne pollen amount) using Generalized Linear Mixed Model (GLMM with Gaussian family and identity link)) (see Appendix S3 for more details). Using the last 22 survey sites represented by a circle, hypothesis tests and analyses of deviance have been performed to test the robustness of the periods and weather variables identified with the GLMM. The corresponding GPS coordinates are indicated in Table S1.

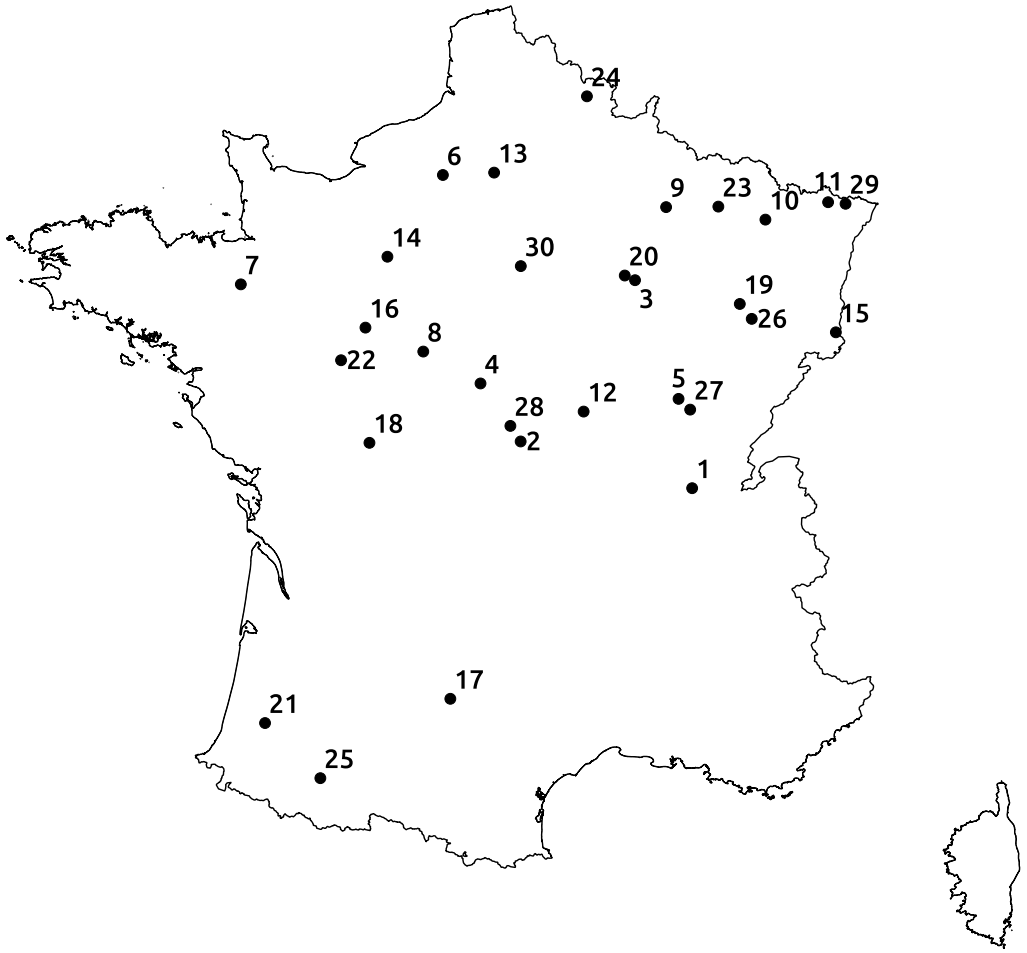

Fig. S2: Spatial distribution of the 30 survey acorn-sampling sites made by the RENECOFOR (Réseau National de suivi à long terme des ECOsystèmes FORestiers de l'ONF (Office National des Forêts)) in France. The characteristics of the acorn-sampling sites are indicated in the Table S2.

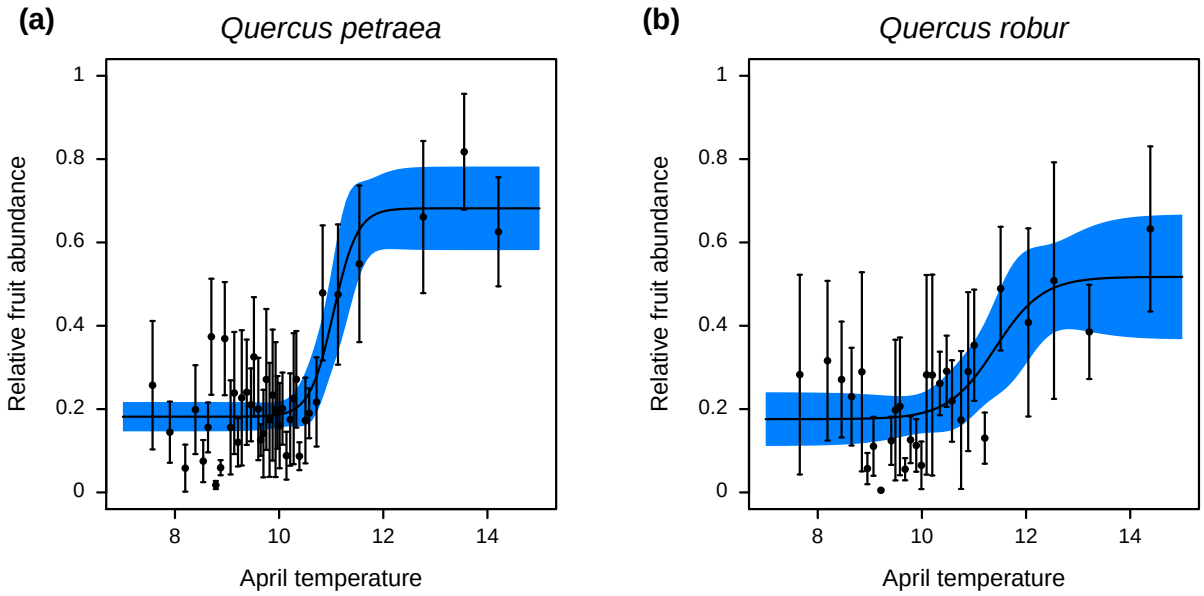

Fig. S3: Logistic response of the acorn production to the April mean Temperature (AT) for *Quercus petraea* (**a**) and *Q. robur* (**b**). The fitted acorn data were computed as relative fruit abundance (i.e., the ratio of the value at any given year at one site to the maximum value ever found at that site). The acorn data collected yearly for 14 years at each of the 19 sites for *Q. petraea* and 9 sites for *Q. robur* (see Table S2) were ranked according to their corresponding AT values, then sets of 6 consecutive values for *Q. petraea* and 4 for *Q. robur* were made to compute means and SD (black dots and their interval segments). Shaded areas show the 95% confidence interval of the model estimates.

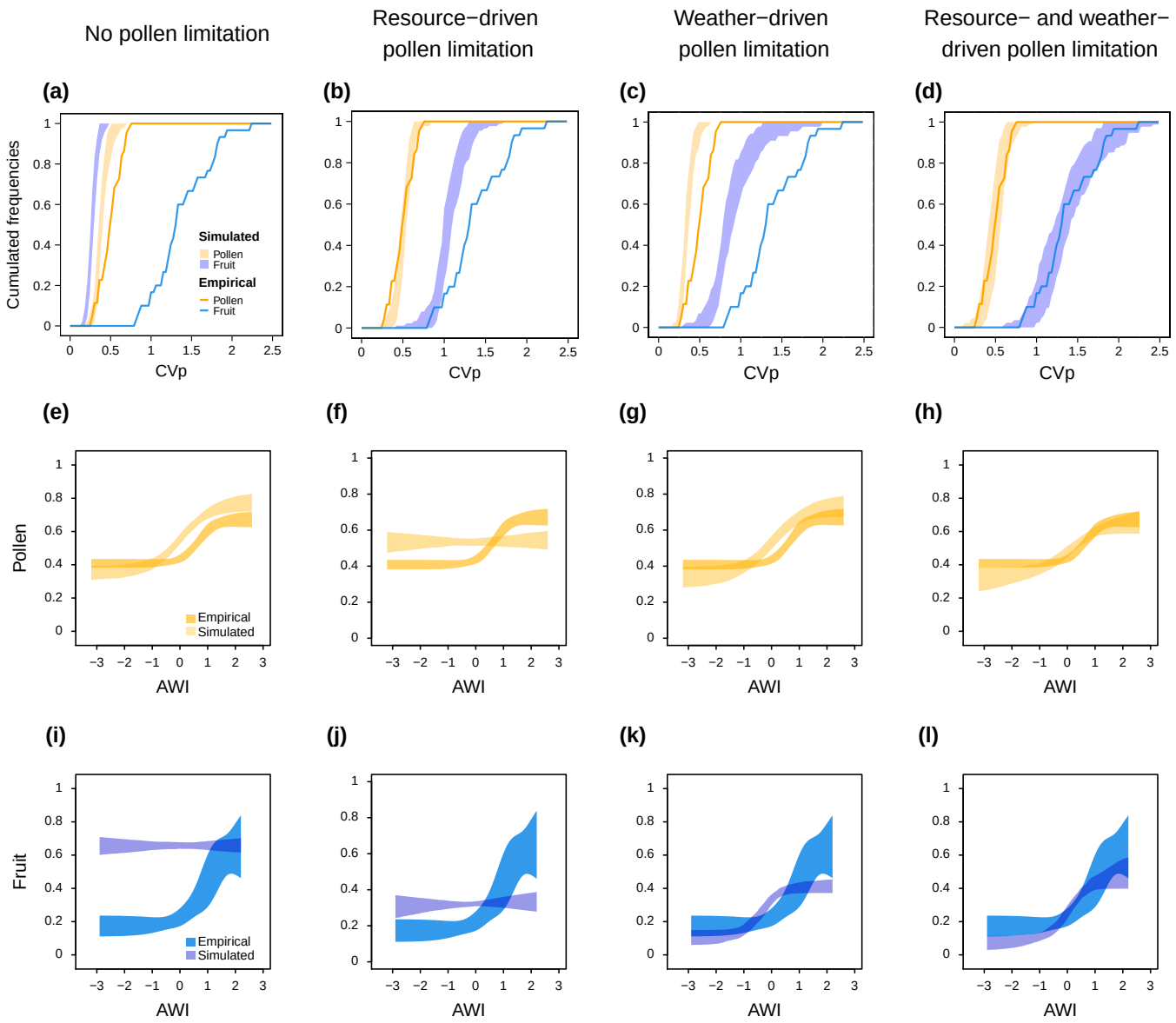

Fig. S4: Model outputs compared to empirical datasets for oak airborne pollen amounts and acorn production. Same legend as Fig. 4 in main text, except for the x-axis of the panels **e-k** for which April Weather Index (AWI) replaced April mean Temperature (AT).

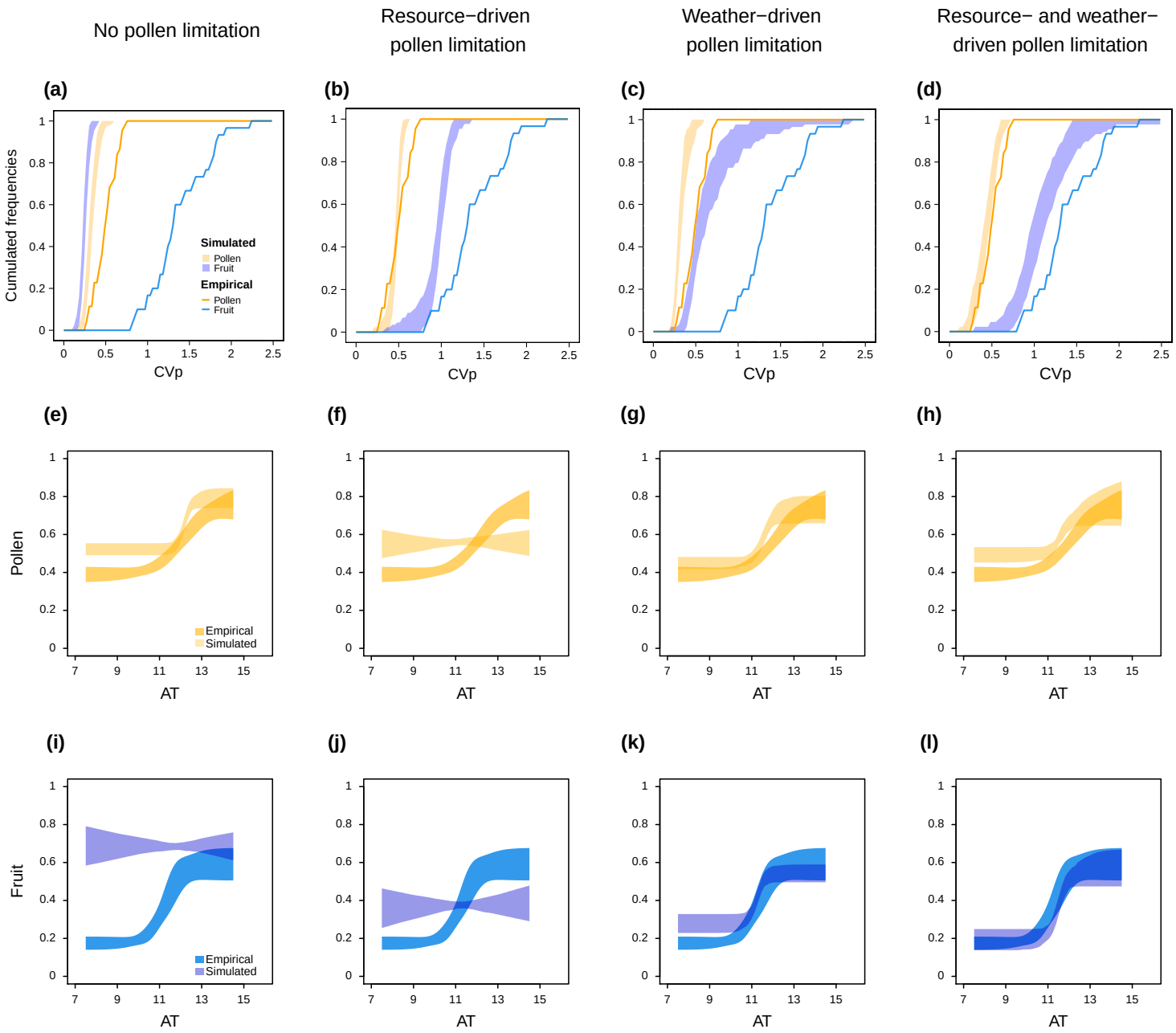

Fig. S5: Model outputs compared to empirical datasets for oak airborne pollen amounts and acorn production, with 2 as the DC average value. Same legend as Fig. 4 in main text.

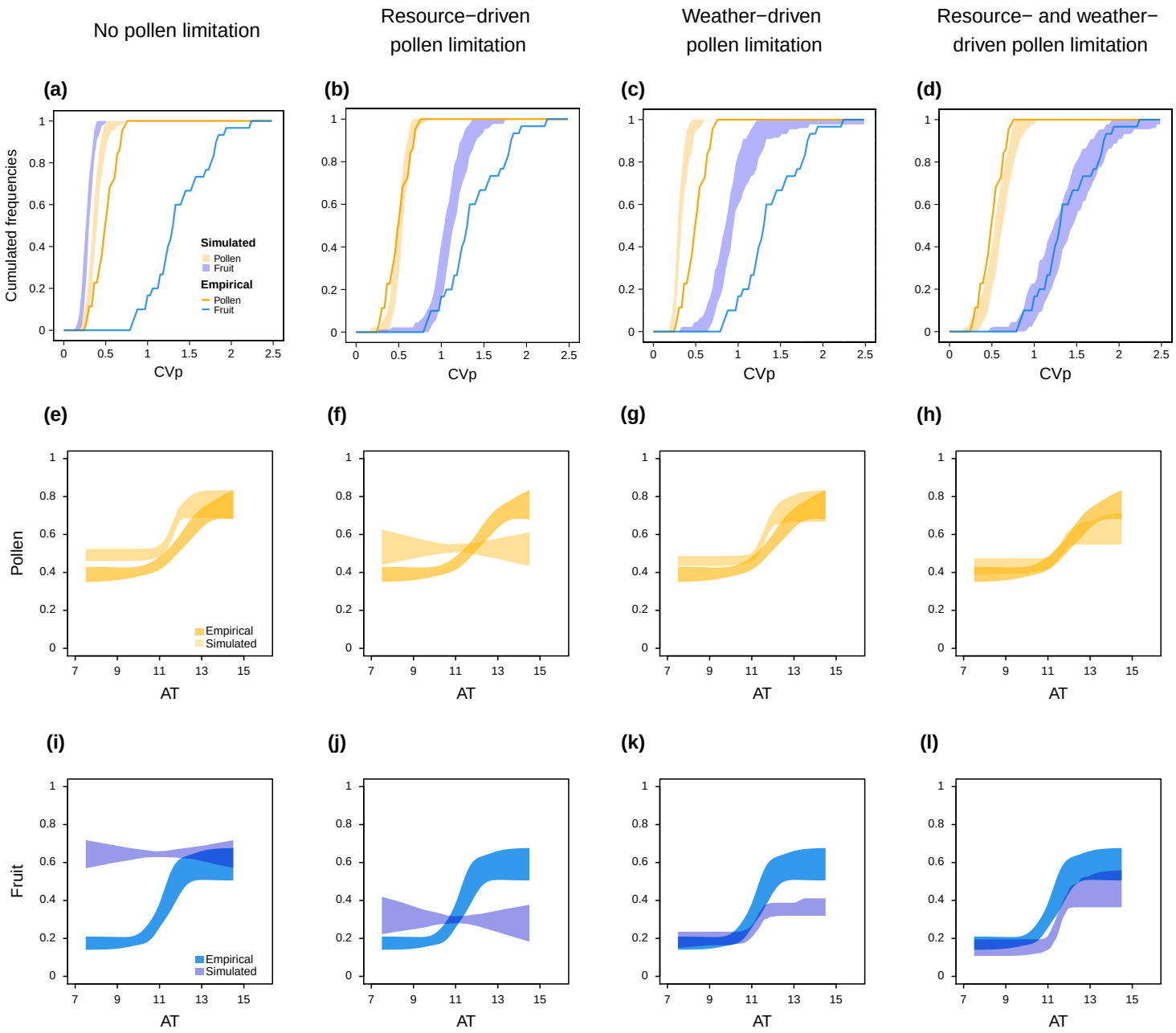

Fig. S6: Model outputs compared to empirical datasets for oak airborne pollen amounts and acorn production, with 8 as the DC average value. Same legend as Fig. 4 in main text.

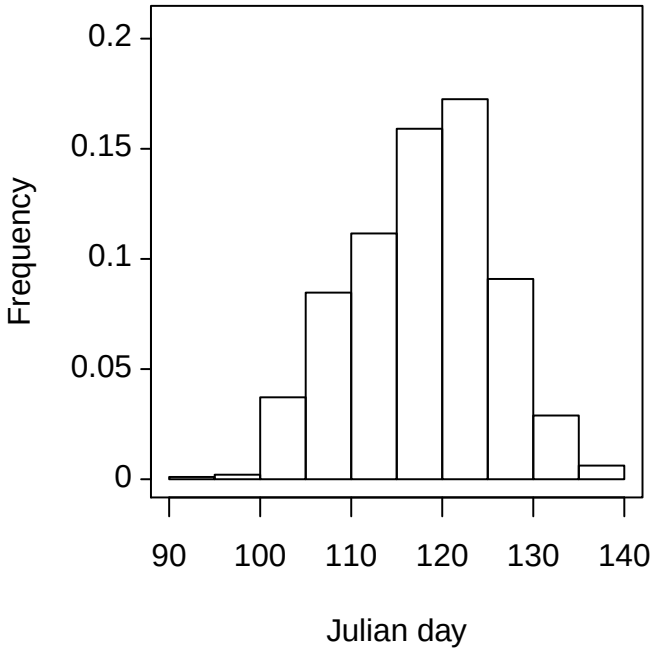

Fig. S7: Distribution of the median date of the oak pollen released each year (1994-2015) at each of the 44 surveyed pollen-sampling sites. The median date is calculated in Julian Day (i.e., the number of days from January 1st of each year). Median dates mostly occurred in second half of April (the interquartile range corresponding to 113 and 124 Julian days).

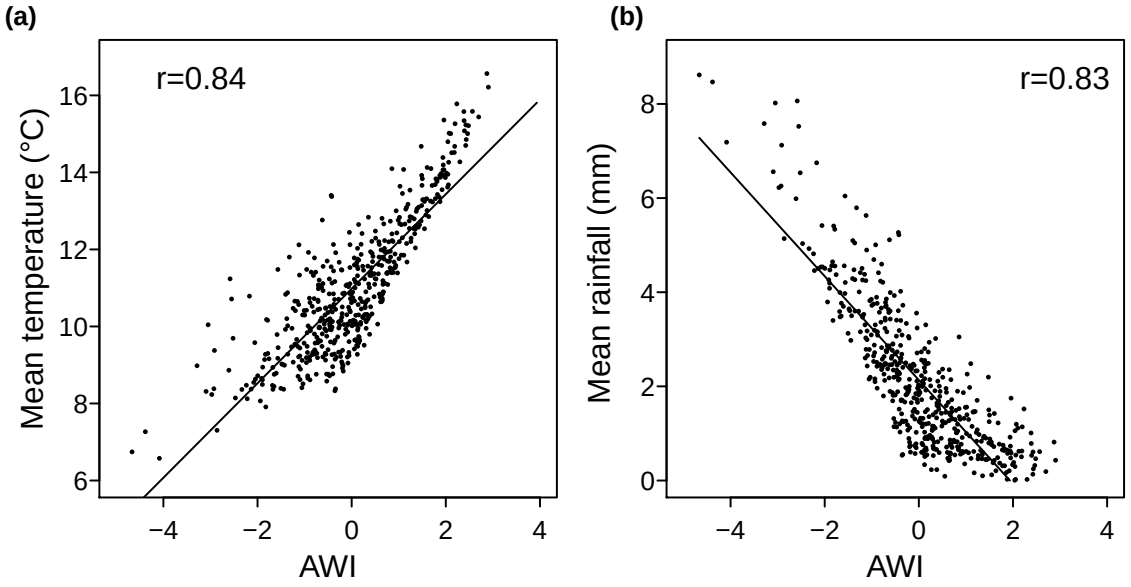

Fig. S8: Relationships between the April Weather Index (AWI) and each of two weather variables: (**a**) mean temperature (°C) and (**b**) rainfall (mm) in April. Each point represent one year at one site (518 *site·year* combinations).

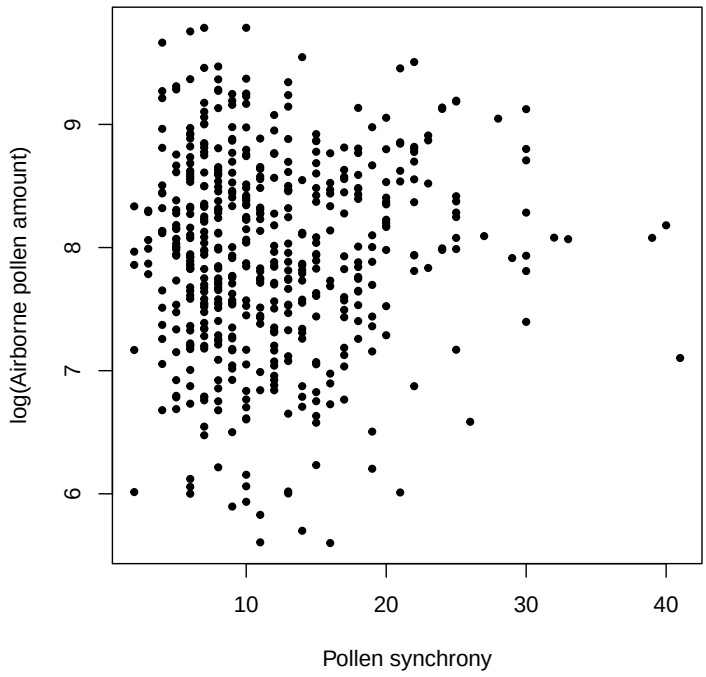

Fig. S9: Non significant relationship between the annual oak airborne pollen amount and pollen synchrony (i.e., the number of days corresponding to the interquartile range of the cumulated daily airborne pollen amount used as a proxy of the duration of the seasonal spreading of airborne pollen and then as a proxy of the synchrony level of pollen release among trees) ($R^2 = 0.0015$).

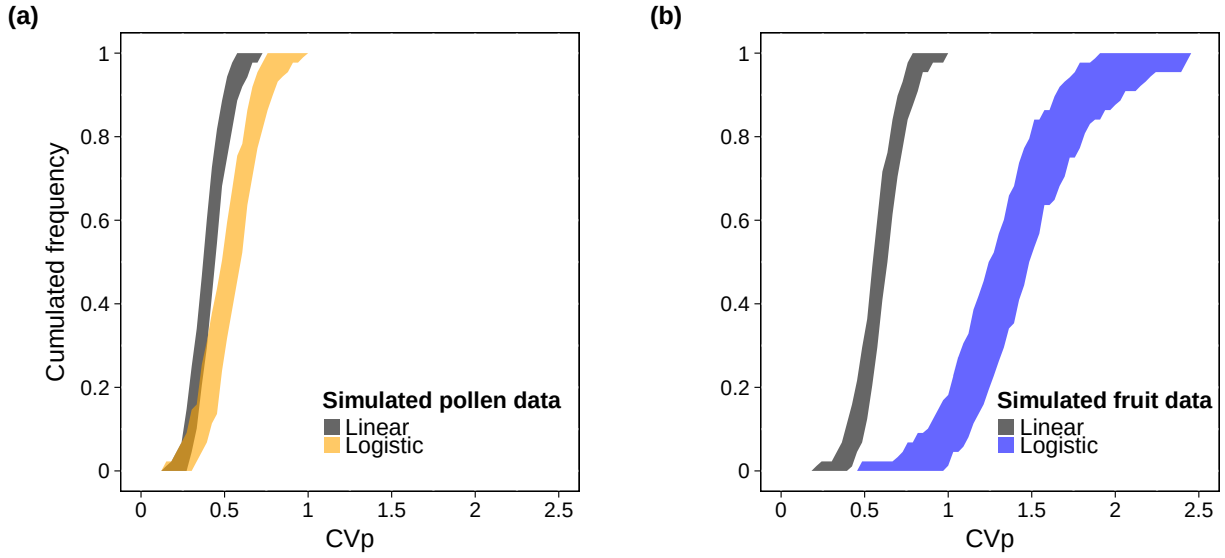

Fig. S10: Effect of the logistic shape of the pollination function that links fruit set to oak airborne pollen amounts on both pollen- and fruit-CVp (population Coefficient of Variation). Venner *et al.* (2016) introduced in their Resource Budget Model (RBM) a logistic shape for the pollination function to capture both dilution and saturation effect at low and high pollen availability, respectively. Here, complementary to their study, we showed that the logistic nature of the pollination function (as compared with linear function) allows generating high increase in the acorn-CVp (**b**) relatively to pollen-CVp (**a**), consistent with field observations (see Fig. 4d in main text).

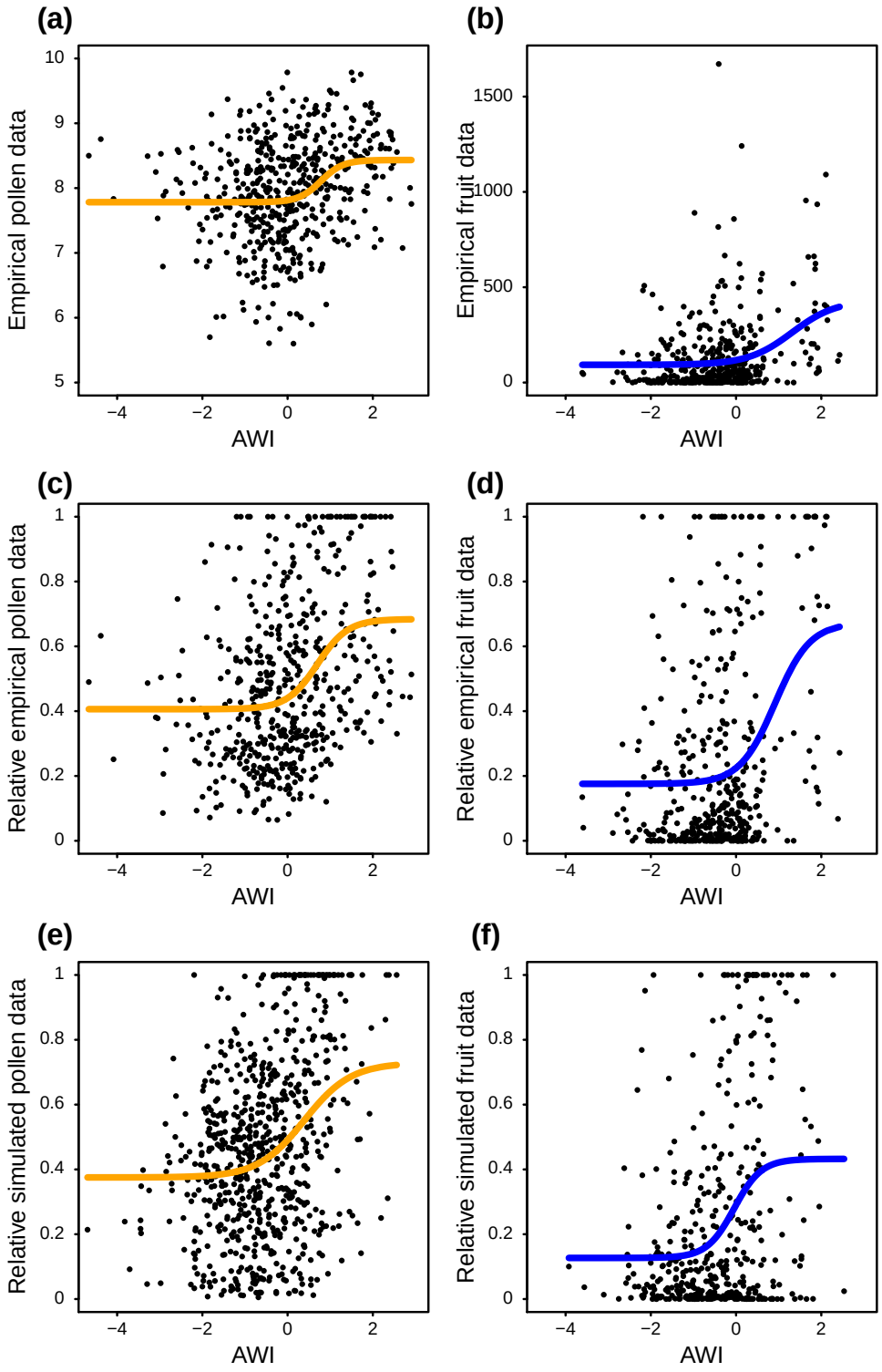

Fig. S11: Comparison between observed and simulated data concerning the impact of spring weather condition on oak airborne pollen amounts and fruit production. The annual airborne pollen amount (**a,c,e**) and fruit production (**b,d,f**) both increased following logistic function with mean April Weather Index (AWI) (**a,b**). Empirical data used in the Generalized Linear Mixed Model (GLMM with Gaussian family and identity link) and Generalized Linear Model (GLM with Gaussian family and identity link) are shown in panels (**a**) and (**b**). For the purpose of comparing empirical and simulated data, we computed relative empirical pollen (or acorn) data (between 0 and 1) by dividing each annual airborne pollen (or acorn) data at a given site by the maximum value recorded at that pollen- (or acorn-) sampling site between 1994 and 2015 (**c, d**). We did the same way for simulated data (**e, f**).

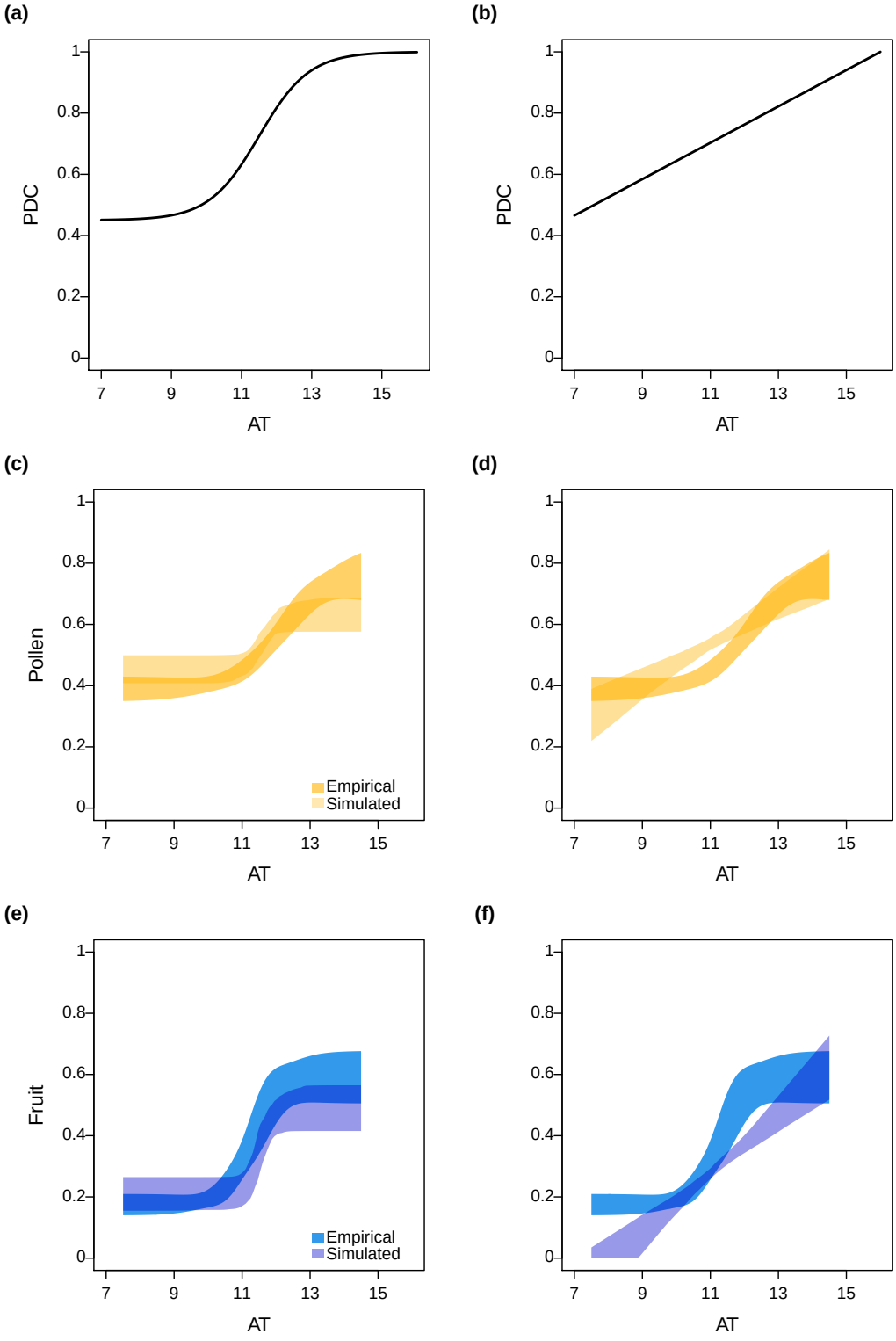

Fig. S12: Effect of April mean Temperature (AT) on the amount of airborne pollen and fruit production, considering either logistic (**a, c, e**) or linear (**b, d, f**) relationship between AT and the Pollen Diffusion Coefficient (PDC) (see equation 6 in Appendix S4). The amount of airborne pollen and fruit production were less sensitive to AT when linear relationship between PDC and pollen was used (**b, d, f**) as compared with the logistic one (**a, c, e**). The logistic response of pollen availability for reproduction to AT might make the fruiting dynamics highly sensitive to even weak variation in spring weather conditions, and thus to climate change.